Supplementary Materials

Ferrocene-bearing Homoleptic and Heteroleptic Paddlewheel-type Dirhodium Complexes

Yusuke Kataoka[1],*, Kozo Sato [1], Natsumi Yano [1,2], and Makoto Handa [1],*

1. Department of Chemistry, Graduate School of Natural Science and Technology, Shimane University, 1060, Nishikawatsu, Matsue, Shimane 690-8504, Japan.
2. Special Course in Science and Engineering, Graduate School of Natural Science and Technology, Shimane University, 1060, Nishikawatsu, Matsue, Shimane 690-8504, Japan.

Contents

Table S1. Averaged bond lengths (Å) of observed and optimized geometries of [Rh$_2$(fca)$_4$(MeOH)$_2$] (**1(MeOH)$_2$**).

	observed geometry	optimized geometry
Rh-Rh	2.377	2.407
Rh-O$_{(fca)}$	2.033	2.066
Rh-O$_{(MeOH)}$	2.283	2.389

Table S2. Averaged bond lengths (Å) of observed and optimized geometries of [Rh$_2$(fca)(piv)$_3$(MeOH)$_2$] (**2(MeOH)$_2$**).

	observed geometry	optimized geometry
Rh-Rh	2.371	2.405
Rh-O$_{(fca)}$	2.031	2.067
Rh-O$_{(trans\text{-}piv)}$	2.030	2.067
Rh-O$_{(cis\text{-}piv)}$	2.027	2.068
Rh-O$_{(MeOH)}$	2.296	2.390

Table S3. TDDFT results (excitation wavelength, oscillator strength, and orbital contribution) of **1(MeOH)₂**.

Excitation state	Wavelength (nm)	Oscillator strength	Orbital contribution
S_1	594.4	0.0043	H-8[π*(Rh₂)]→L[σ*(Rh₂)] (84%), H-10[π*(Rh₂)]→L+1[*anti-bonding*-dx^2-y^2(Rh₂)] (6%), H-4[d(fca)]→L[σ*(Rh₂)] (6%)
S_2	585.5	0.0001	H-6[d(fca)]→L+2[d(fca)] (21%), H-5[d(fca)]→L+7[d(fca)] (16%), H-7[d(fca)]→L+5[delocalization] (7%), H-2[d(fca)]→L+9[d(fca)] (7%), H-7[d(fca)]→L+4[delocalization] (6%), H-6[d(fca)]→L+13[d(fca)] (5%), H-1[d(fca)]→L+5[delocalization] (5%), H[d(fca)]→L+9[d(fca)] (5%)
S_4	584.9	0.0001	H-4[d(fca)]→L+3[d(fca)] (20%), H-3[d(fca)]→L+8[d(fca)] (15%), H[d(fca)]→L+10[d(fca)] (7%), H-1[d(fca)]→L+4[delocalization] (5%), H-2[d(fca)]→L+10[d(fca)] (5%)
S_6	582.9	0.0059	H-10[π*(Rh₂)]→L[σ*(Rh₂)] (23%), H-6[d(fca)]→L+9[d(fca)] (9%), H-2[d(fca)]→L+2[d(fca)] (8%), H-5[d(fca)]→L+5[delocalization] (8%), H[d(fca)]→L+2[d(fca)] (7%) H-5[d(fca)]→L+4[delocalization] (7%), H-7[d(fca)]→L+7[d(fca)] (7%)
S_8	582.1	0.0034	H[d(fca)]→L+3[d(fca)] (10%), H-4[d(fca)]→L+10[d(fca)] (9%), H-1[d(fca)]→L+8[d(fca)] (7%), H-2[d(fca)]→L+3[d(fca)] (7%), H-3[d(fca)]→L+6 [*bonding*-dx^2-y^2(Rh₂)] (7%), H-3[d(fca)]→L+4[delocalization] (7%), H-7[d(fca)]→L+8[d(fca)] (7%)
S_{10}	581.0	0.0006	H-10[π*(Rh₂)]→L[σ*(Rh₂)] (62%), H-8[π*(Rh₂)]→L+1[*anti-bonding*-dx^2-y^2(Rh₂)] (5%)
S_{11}	503.4	0.0019	H-13[d(fca)]→L+5[delocalization] (11%), H-6[d(fca)]→L+9[d(fca)] (11%), H-13[d(fca)]→L+4[delocalization] (9%), H-14[d(fca)]→L+2[d(fca)] (9%),H-7[d(fca)]→L+7[d(fca)] (8%), H-1[d(fca)]→L+7[d(fca)] (5%), H-15[d(fca)]→L+2[d(fca)] (5%)
S_{14}	503.1	0.0018	H-4[d(fca)]→L+10[d(fca)] (10%), H-14[d(fca)]→L+3[d(fca)] (9%), H-12[d(fca)]→L+6[*bonding*-dx^2-y^2(Rh₂)] (8%), H-12[d(fca)]→L+4[delocalization] (8%), H-1[d(fca)]→L+8[d(fca)] (7%), H-7[d(fca)]→L+8[d(fca)] (7%), H-12[d(fca)]→L+5[delocalization] (5%), H-15[d(fca)]→L+3[d(fca)] (5%)
S_{16}	492.8	0.0001	H-13[d(fca)]→L+7[d(fca)] (20%), H-5[d(fca)]→L+7[d(fca)] (19%), H-2[d(fca)]→L+9[d(fca)] (10%), H-14[d(fca)]→L+9[d(fca)] (9%), H-6[d(fca)]→L+2[d(fca)] (6%), H[d(fca)]→L+9[d(fca)] (5%)
S_{22}	432.3	0.0026	H-8[π*(Rh₂)]→L+1[*anti-bonding*-dx^2-y^2(Rh₂)] (80%), H-10[π*(Rh₂)]→L[σ*(Rh₂)] (8%), H-4[d(fca)]→L+1[*anti-bonding*-dx^2-y^2(Rh₂)] (6%)

S_{23}	424.9	0.0028	H-10[π*(Rh$_2$)]→L+1[*anti-bonding*-dx^2-y^2(Rh$_2$)] (86%), H-8[π*(Rh$_2$)]→L[σ*(Rh$_2$)] (6%)
S_{26}	379.7	0.0017	H-6[d(fca)]→L+9[d(fca)] (11%), H-13[d(fca)]→L+5[delocalization] (9%), H-7[d(fca)]→L+7[d(fca)] (9%), H-14[d(fca)]→L+2[d(fca)] (8%), H-13[d(fca)]→L+4[delocalization] (8%), H-2[d(fca)]→L+2[d(fca)] (6%), H-1[d(fca)]→L+7[d(fca)] (6%), H[d(fca)]→L+2[d(fca)] (5%), H-5[d(fca)]→L+4[delocalization] (5%), H-5[d(fca)]→L+5[delocalization] (5%), H-11[δ(Rh$_2$)]→L+2[d(fca)] (5%)
S_{28}	379.4	0.0017	H-4[d(fca)]→L+10[d(fca)] (10%), H-14[d(fca)]→L+3[d(fca)] (8%), H-7[d(fca)]→L+8[d(fca)] (7%), H-12[d(fca)]→L+4[delocalization] (7%), H-1[d(fca)]→L+8[d(fca)] (7%), H-12[d(fca)]→L+6[*bonding*-dx^2-y^2(Rh$_2$)] (7%), H[d(fca)]→L+3[d(fca)] (6%), H-2[d(fca)]→L+3[d(fca)] (5%), H-11[δ(Rh$_2$)]→L+3[d(fca)] (5%)
S_{32}	367.5	0.0003	H-13[d(fca)]→L+7[d(fca)] (23%), H-14[d(fca)]→L+9[d(fca)] (13%), H-5[d(fca)]→L+7[d(fca)] (11%), H-6[d(fca)]→L+2[d(fca)] (9%), H-2[d(fca)]→L+9[d(fca)] (6%), H-15[d(fca)]→L+10[d(fca)] (5%)
S_{38}	357.3	0.0018	H-4[d(fca)]→L[σ*(Rh$_2$)] (89%), H-8[π*(Rh$_2$)]→L[σ*(Rh$_2$)] (6%)
S_{39}	357.2	0.0019	H-6[d(fca)]→L[σ*(Rh$_2$)] (94%)
S_{44}	322.0	0.0001	H[d(fca)]→L+1[*anti-bonding*-dx^2-y^2(Rh$_2$)] (89%)
S_{49}	316.5	0.0044	H-4[d(fca)]→L+1[*anti-bonding*-dx^2-y^2(Rh$_2$)] (89%), H-8[π*(Rh$_2$)]→L+1[*anti-bonding*-dx^2-y^2(Rh$_2$)] (6%)
S_{50}	316.4	0.0044	H-6[d(fca)]→L+1[*anti-bonding*-dx^2-y^2(Rh$_2$)] (94%)
S_{56}	310.0	0.0002	H-10[π*(Rh$_2$)]→L+2[d(fca)] (74%), H-8[π*(Rh$_2$)]→L+2[d(fca)] (18%)
S_{58}	307.8	0.0001	H-10[π*(Rh$_2$)]→L+3[d(fca)] (85%), H-8[π*(Rh$_2$)]→L+3[d(fca)] (8%)
S_{60}	303.0	0.0036	H-6[d(fca)]→L+13[d(fca)] (23%), H-6[d(fca)]→L+2[d(fca)] (18%), H-6[d(fca)]→L+12[d(fca)] (11%), H-7[d(fca)]→L+14[d(fca)] (11%), H-1[d(fca)]→L+14[d(fca)] (8%), H-7[d(fca)]→L+16[d(fca)] (7%), H-1[d(fca)]→L+16[d(fca)] (5%)
S_{62}	302.1	0.0037	H-4[d(fca)]→L+3[d(fca)] (17%), H-4[d(fca)]→L+12[d(fca)] (16%), H-4[d(fca)]→L+13[d(fca)] (10%), H-7[d(fca)]→L+14[d(fca)] (7%), H-7[d(fca)]→L+16[d(fca)] (7%), H-4[d(fca)]→L+15[d(fca)] (7%), H-1[d(fca)]→L+14[d(fca)] (7%), H-1[d(fca)]→L+16[d(fca)] (9%)
S_{65}	300.0	0.0024	H-9[δ*(Rh$_2$)]→L+4[delocalization] (53%), H-1[d(fca)]→L+4[delocalization] (21%), H-16[σ(Rh$_2$)]→L[σ*(Rh$_2$)] (9%)

Table S4. TDDFT results (excitation wavelength, oscillator strength, and orbital contribution) of **2(MeOH)$_2$**.

Excitation state	Wavelength (nm)	Oscillator strength	Orbital contribution
S$_1$	594.4	0.0038	H-2[π*(Rh$_2$)]→L[σ*(Rh$_2$)] (85%), H-3[π*(Rh$_2$)]→L+1[*anti-bonding*-dx^2-y^2(Rh$_2$)] (6%), H-1[d(fca)]→L[σ*(Rh$_2$)] (5%)
S$_2$	583.9	0.0001	H-1[d(fca)]→L+2[d(fca)] (33%), H[d(fca)]→L+4[d(fca)] (32%), H-1[d(fca)]→L+6[d(fca)] (10%), H-1[d(fca)]→L+3[*bonding*-dx^2-y^2(Rh$_2$)] (9%)
S$_3$	583.2	0.003	H-3[π*(Rh$_2$)]→L[σ*(Rh$_2$)](82%), H-2[π*(Rh$_2$)]→L+1[*anti-bonding*-dx^2-y^2(Rh$_2$)] (7%)
S$_4$	580.7	0.0012	H[d(fca)]→L+2[d(fca)] (33%), H-1[d(fca)]→L+4[d(fca)] (32%), H[d(fca)]→L+6[d(fca)] (12%), H[d(fca)]→L+3[*bonding*-dx^2-y^2(Rh$_2$)] (10%)
S$_5$	502.4	0.0008	H-5[d(fca)]→L+2[d(fca)] (28%), H-1[d(fca)]→L+4[d(fca)] (26%), H-5[d(fca)]→L+6[d(fca)] (11%), H[d(fca)]→L+2[d(fca)] (9%), H-5[d(fca)]→L+3[*bonding*-dx^2-y^2(Rh$_2$)] (8%)
S$_{10}$	433.9	0.002	H-2[π*(Rh$_2$)]→L+1[*anti-bonding*-dx^2-y^2(Rh$_2$)] (82%), H-3[π*(Rh$_2$)]→L[σ*(Rh$_2$)](8%)
S$_{11}$	427.4	0.0024	H-3[π*(Rh$_2$)]→L+1[*anti-bonding*-dx^2-y^2(Rh$_2$)] (83%), H-2[π*(Rh$_2$)]→L[σ*(Rh$_2$)](7%)
S$_{14}$	378.8	0.0007	H-5[d(fca)]→L+2[d(fca)] (27%), H-1[d(fca)]→L+4[d(fca)] (27%), H[d(fca)]→L+2[d(fca)] (17%), H-5[d(fca)]→L+6[d(fca)] (7%), H-5[d(fca)]→L+3[*bonding*-dx^2-y^2(Rh$_2$)] (7%)
S$_{15}$	367.0	0.0001	H-5[d(fca)]→L+4[d(fca)] (50%), H[d(fca)]→L+4[d(fca)] (24%), H-1[d(fca)]→L+2[d(fca)] (14%)
S$_{17}$	354.8	0.0009	H-1[d(fca)]→L[σ*(Rh$_2$)](84%), H-4[δ*(Rh$_2$)]→L[σ*(Rh$_2$)] (8%), H-2[π*(Rh$_2$)]→L[σ*(Rh$_2$)](5%)
S$_{20}$	320.3	0.0001	H-11[π(Rh$_2$)]→L[σ*(Rh$_2$)](73%), H-9[π(Rh$_2$)]→L[σ*(Rh$_2$)](7%), H-2[π*(Rh$_2$)]→L+2[d(fca)] (6%)
S$_{22}$	315.4	0.0021	H-1[d(fca)]→L+1[*anti-bonding*-dx^2-y^2(Rh$_2$)] (85%), H-4[δ*(Rh$_2$)]→L+1[*anti-bonding*-dx^2-y^2(Rh$_2$)] (7%), H-2[π*(Rh$_2$)]→L+1[*anti-bonding*-dx^2-y^2(Rh$_2$)] (5%)
S$_{24}$	303.5	0.0002	H-3[π*(Rh$_2$)]→L+2[d(fca)] (58%), H-3[π*(Rh$_2$)]→L+3[*bonding*-dx^2-y^2(Rh$_2$)] (19%), H-2[π*(Rh$_2$)]→L+2[d(fca)] (12%)
S$_{25}$	302.5	0.0017	H-4[δ*(Rh$_2$)]→L+2[d(fca)] (47%), H-1[d(fca)]→L+2[d(fca)] (13%), H-1[d(fca)]→L+6[d(fca)] (10%), H-4[δ*(Rh$_2$)]→L+3[*bonding*-dx^2-y^2(Rh$_2$)] (10%), H-3[π*(Rh$_2$)]→L+2[d(fca)] (6%)
S$_{26}$	300.6	0.0005	H-1[d(fca)]→L+6[d(fca)] (35%), H-4[δ*(Rh$_2$)]→L+2[d(fca)] (24%), H-1[d(fca)]→L+2[d(fca)] (10%), H-4[δ*(Rh$_2$)]→L+6[d(fca)] (5%), H-1[d(fca)]→L+5[d(fca)] (6%)

Table S5. Selected bond lengths (Å) and angles (°) of **1(MeOH)₂**.

bond lengths (Å)			
Rh1-Rh1′	2.3771(3)	Fe1-C7	2.045(2)
Rh1-O1	2.0226(13)	Fe1-C8	2.040(2)
Rh1-O2	2.0466(13)	Fe1-C9	2.044(2)
Rh1-O3	2.0131(12)	Fe1-C10	2.046(2)
Rh1-O4	2.0502(12)	Fe1-C11	2.043(2)
Rh1-O5	2.2839(14)	Fe2-C13	2.0219(18)
C1-O1	1.267(2)	Fe2-C14	2.036(2)
C1-O2	1.275(2)	Fe2-C15	2.056(2)
C12-O3	1.264(2)	Fe2-C16	2.0678(19)
C12-O4	1.277(2)	Fe2-C17	2.0456(19)
Fe1-C2	2.0380(18)	Fe2-C18	2.042(2)
Fe1-C3	2.0484(19)	Fe2-C19	2.037(2)
Fe1-C4	2.0488(19)	Fe2-C20	2.043(2)
Fe1-C5	2.038(2)	Fe2-C21	2.046(2)
Fe1-C6	2.033(2)	Fe2-C22	2.044(2)
bond angles (°)			
Rh1-Rh1′-O1′	89.32(4)	Rh1-Rh1′-O5′	173.96(4)
Rh1-Rh1′-O2	87.53(4)	O1-C1-O2	126.01(17)
Rh1-Rh1′-O3′	88.24(4)	O3-C12-O4	125.97(17)
Rh1-Rh1′-O4	88.55(4)		

Table S6. Selected bond lengths (Å) and angles (°) of **2(MeOH)₂**.

| bond lengths (Å)					
Rh1-Rh2	2.3712(3)	Fe1-C3	2.021(4)	C29-O11	1.267(4)
Rh1-O1	2.029(2)	Fe1-C4	2.042(5)	C29-O12	1.268(4)
Rh2-O2	2.044(2)	Fe1-C5	2.048(4)	C40-O13	1.266(4)
Rh1-O3	2.025(2)	Fe1-C6	2.042(4)	C40-O14	1.272(4)
Rh2-O4	2.029(2)	Fe1-C7	1.988(5)	C45-O15	1.265(4)
Rh1-O5	2.020(2)	Fe1-C8	1.998(5)	C45-O16	1.273(4)
Rh2-O6	2.031(3)	Fe1-C9	2.019(5)	C50-O17	1.263(4)
Rh1-O7	2.033(2)	Fe1-C10	2.034(4)	C50-O18	1.267(4)
Rh2-O8	2.029(2)	Fe1-C11	2.011(4)	Fe2-C30	2.010(4)
Rh1-O9	2.285(2)	Rh3-Rh4	2.3724(3)	Fe2-C31	2.029(4)
Rh2-O10	2.310(2)	Rh3-O11	2.036(3)	Fe2-C32	2.044(4)
C1-O1	1.262(4)	Rh4-O12	2.015(3)	Fe2-C33	2.044(4)
C1-O2	1.283(4)	Rh3-O13	2.025(2)	Fe2-C34	2.024(4)
C12-O3	1.272(4)	Rh4-O14	2.031(2)	Fe2-C35	2.019(4)
C12-O4	1.258(4)	Rh3-O15	2.033(2)	Fe2-C36	2.027(4)
C17-O5	1.262(4)	Rh4-O16	2.036(2)	Fe2-C37	2.040(4)
C17-O6	1.267(4)	Rh3-O17	2.008(2)	Fe2-C38	2.053(4)
C22-O7	1.260(4)	Rh4-O18	2.038(2)	Fe2-C39	2.042(4)
C22-O8	1.275(4)	Rh3-O19	2.292(2)		
Fe1-C2	2.021(3)	Rh4-O20	2.297(3)		
bond angles (°)					
Rh1-Rh2-O2		88.34(6)	Rh3-Rh4-O12		88.56(7)
Rh1-Rh2-O4		88.20(7)	Rh3-Rh4-O14		87.85(7)
Rh1-Rh2-O6		87.61(7)	Rh3-Rh4-O16		88.52(6)
Rh1-Rh2-O8		88.07(7)	Rh3-Rh4-O18		87.39(6)
Rh2-Rh1-O1		88.33(7)	Rh4-Rh3-O11		88.16(7)
Rh2-Rh1-O3		88.28(7)	Rh4-Rh3-O13		88.65(7)
Rh2-Rh1-O5		88.80(7)	Rh4-Rh3-O15		87.78(6)
Rh2-Rh1-O7		88.21(7)	Rh4-Rh3-O17		89.03(7)
Rh1-Rh2-O10		178.38(7)	Rh3-Rh4-O20		177.59(7)
Rh2-Rh1-O9		176.86(7)	Rh4-Rh3-O19		174.90(7)
O1-C1-O2		124.6(3)	O11-C29-O12		125.9(3)
O3-C12-O4		125.3(3)	O13-C40-O14		124.8(3)
O5-C17-O6		125.1(4)	O15-C45-O16		124.2(3)
O7-C22-O8		124.2(3)	O17-C50-O18		125.2(3)
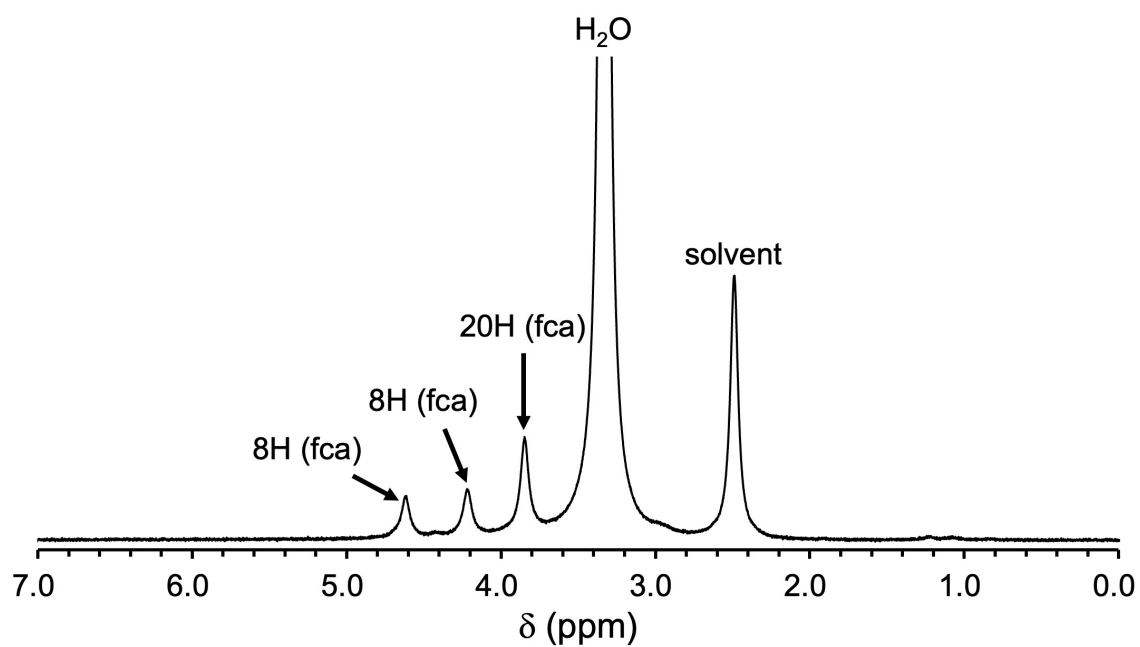
Figure S1. ^1H NMR spectrum of **1** in DMSO-d_6.
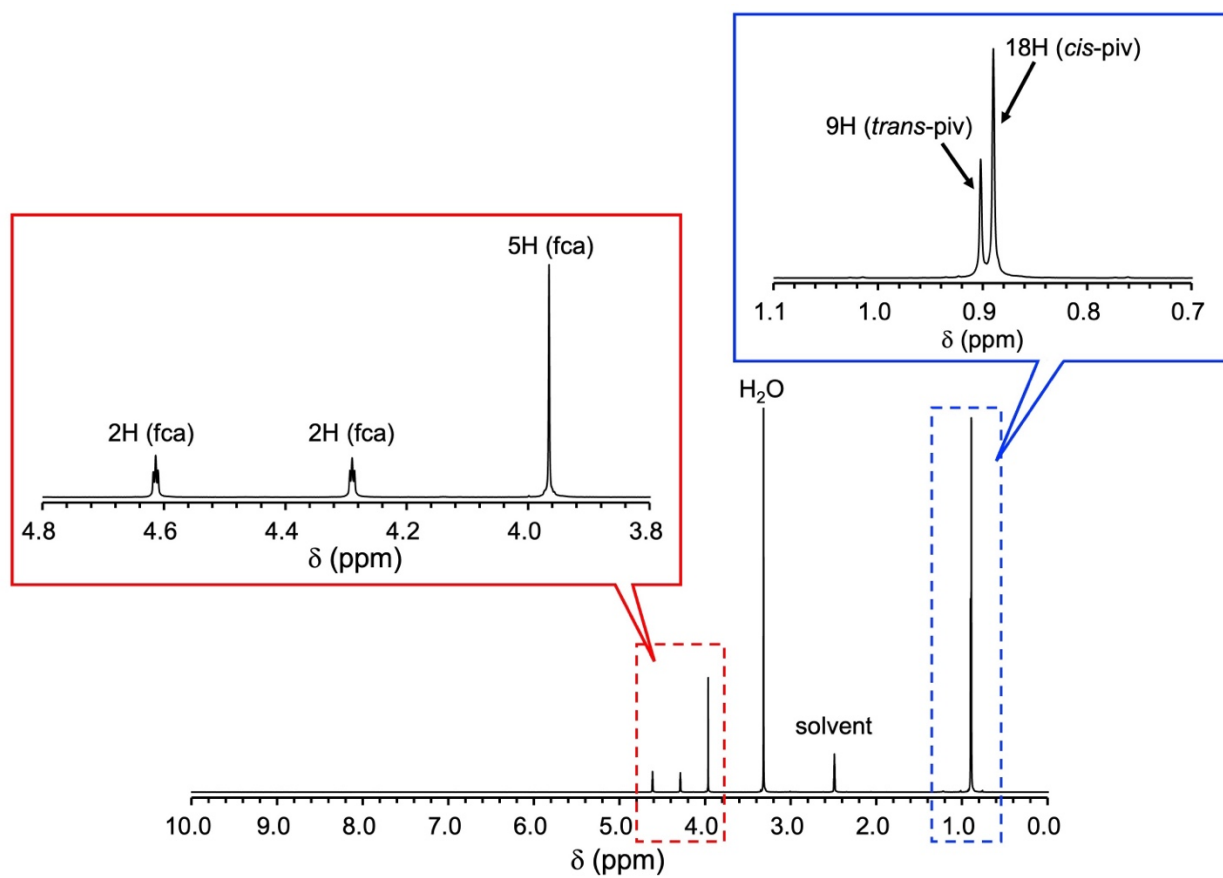
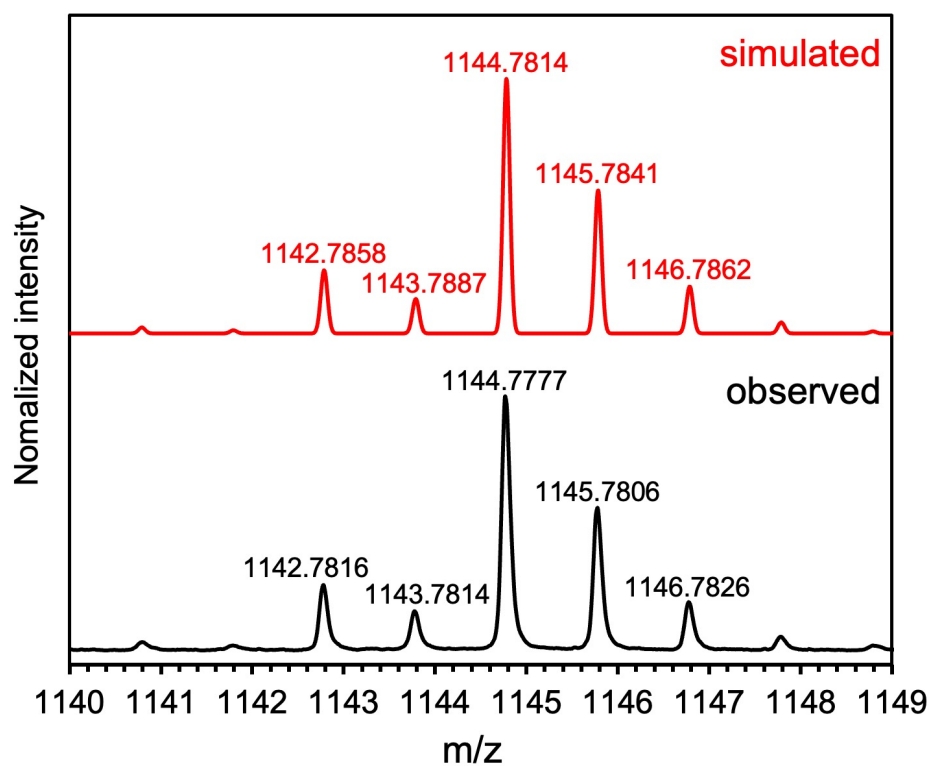Figure S2. ^1H NMR spectrum of **2** in DMSO-d_6.

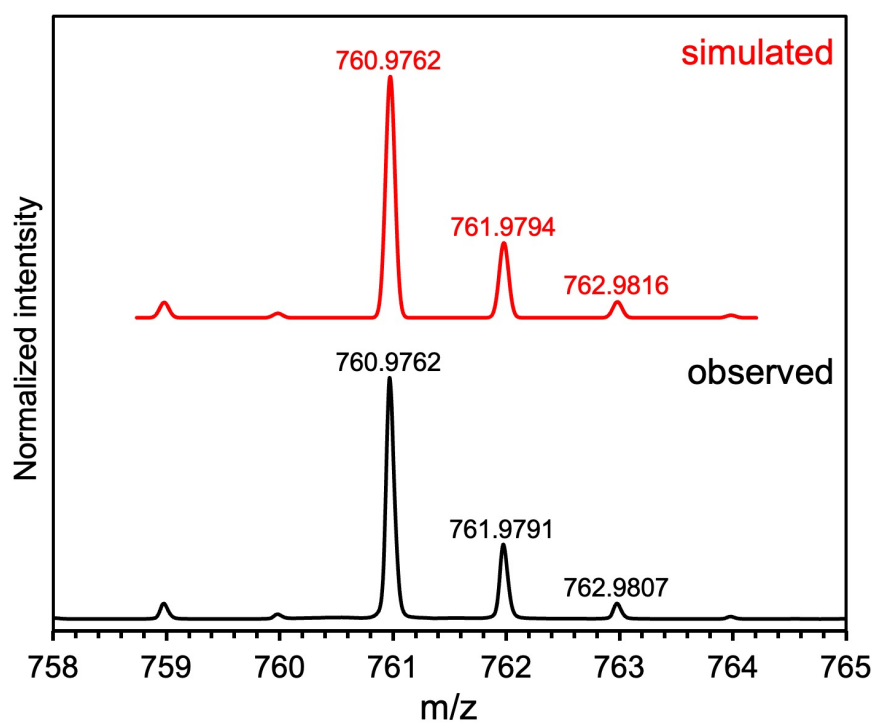Figure S3. Observed and simulated ESI-TOF-MS spectra of **1**.

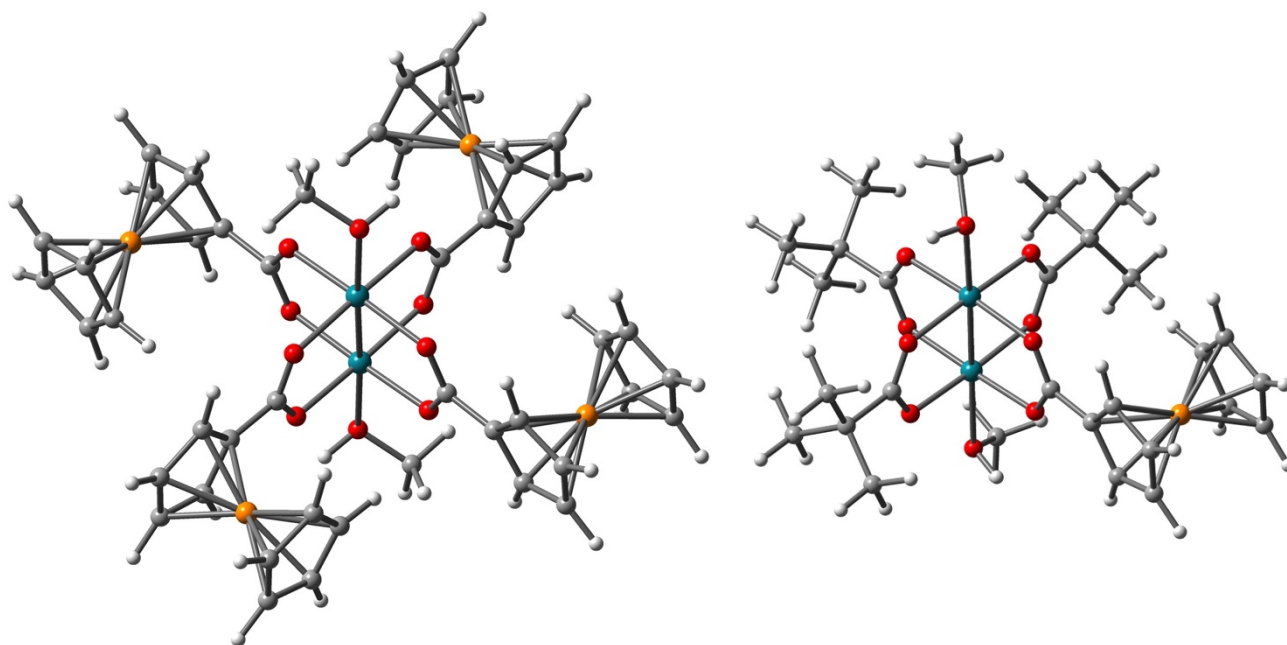Figure S4. Observed and simulated ESI-TOF-MS spectra of **2**.

Figure S5. Optimized geometries of **1(MeOH)₂** (left) and **2(MeOH)₂** (right).
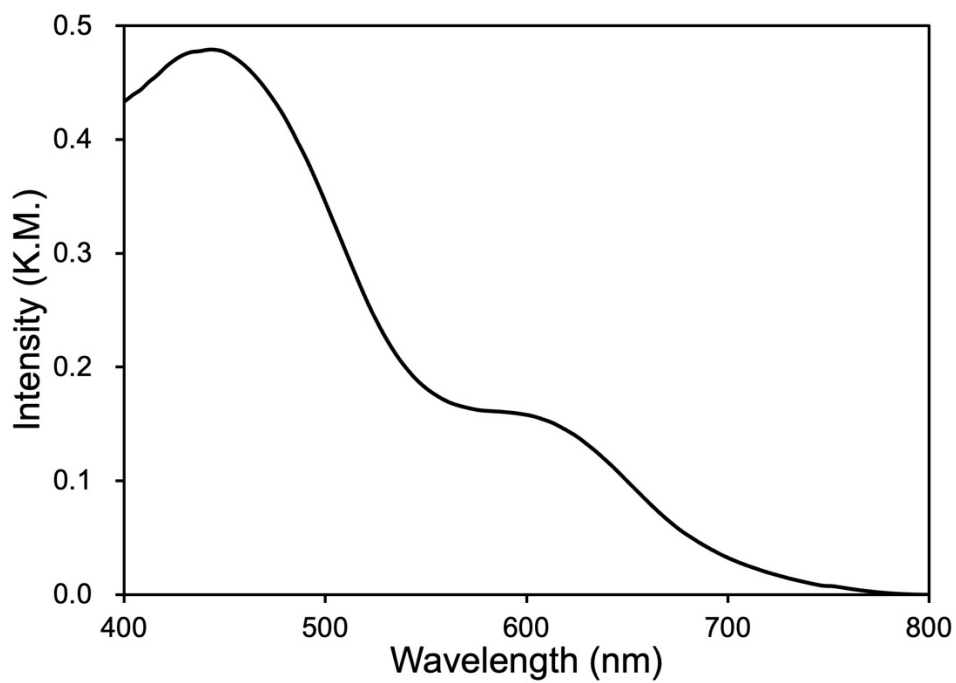

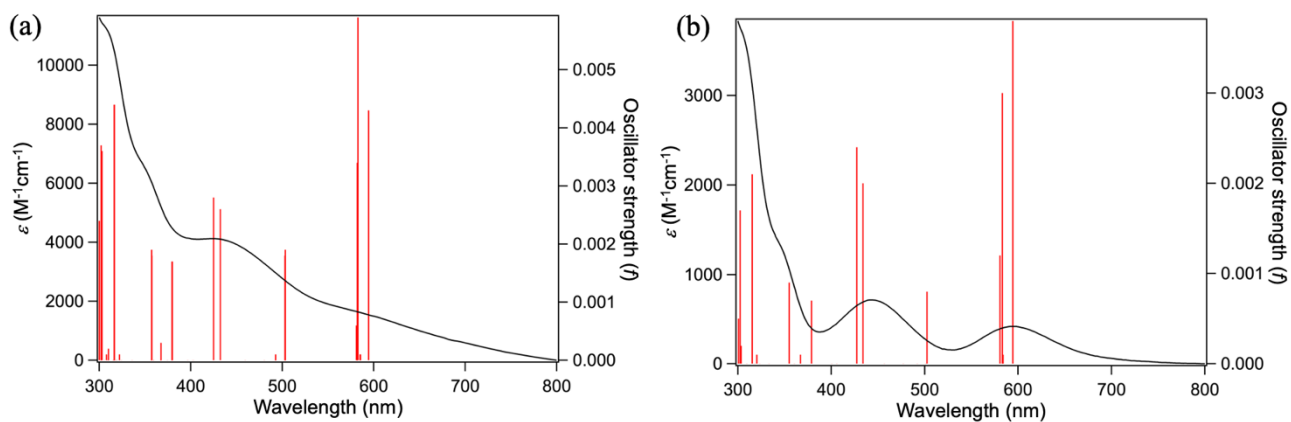Figure S6. Diffuse reflectance (DR) spectrum of **1**.

Figure S7. Observed spectra (black line) and calculated vertical excitations (red line) of (a) **1(MeOH)₂** and (b) **2(MeOH)₂**.
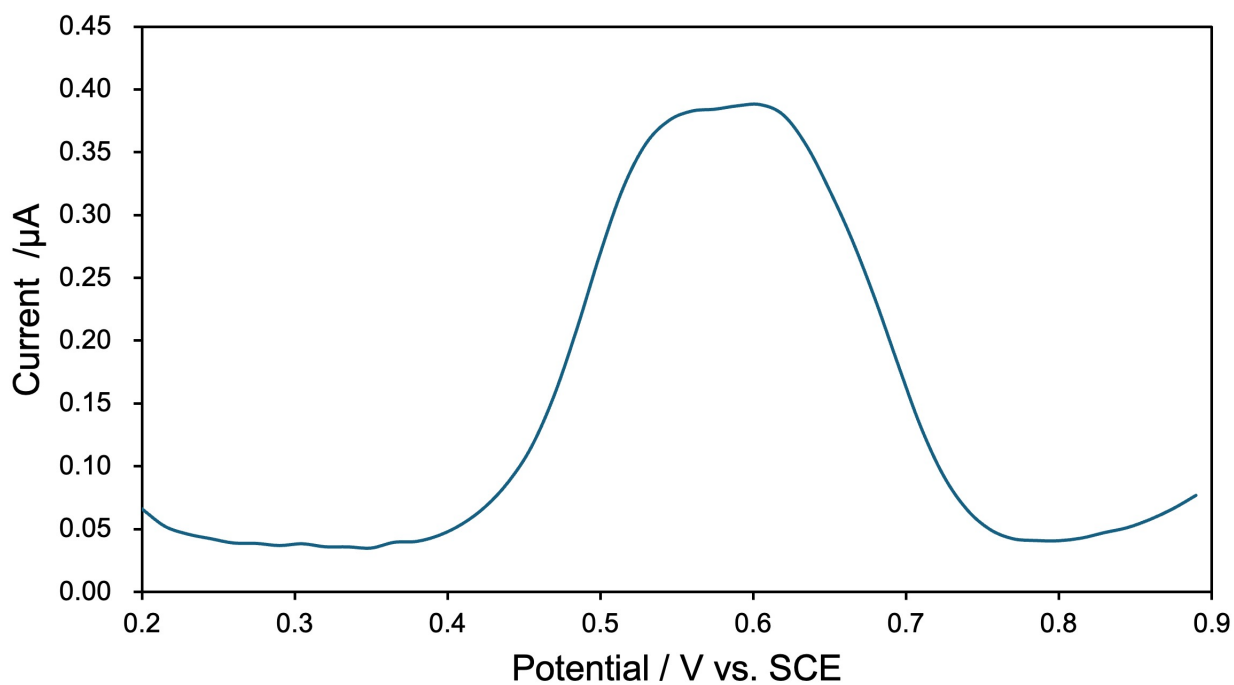

Figure S8. Differential pulse voltammetry (DPV) diagram of **1** (0.10 mM) in 9:1 CHCl₃-MeOH solution containing 0.10 M TBAPF₆.